JOURNAL OF SOLID STATE CHEMISTRY **22,** 331–340 (1977)

Phase Relations in the Dioxide–Trioxide Region of Some 3*d* Transition Metal–W–O Ternary Systems

THOMMY EKSTRÖM

Department of Inorganic Chemistry, Arrhenius Laboratory, University of Stockholm, S-104 05 Stockholm, Sweden

AND R. J. D. TILLEY

School of Materials Science, University of Bradford, Bradford BD7 1DP, West Yorkshire, England

Received February 22, 1977; revised May 17, 1977

The phases occurring in the Mn–W–O, Fe–W–O, Co–W–O, and Ni–W–O systems at 1373°K have been determined using X-ray diffraction and electron and optical microscopy. Experimentally most attention was given to the Mn–W–O system, where it was found that Mn entered as the Mn^{2+} ion into the WO_3 host matrix and formed a perovskite-related bronze Mn_xWO_3. The highest observed x-value in the bronze is about 0.027. In addition a metastable $\theta_w(Mn)$ oxide with the Mo_5O_{14} structure and a disordered oxide of overall composition approximately $(Mn, W)O_{2.82}$ were found. The Fe–W–O system was similar to the Mn–W–O system but significant differences occurred in the Co–W–O and Ni–W–O systems where M_xWO_3 bronze phases were not observed to form at 1373°K. The stability of the M_xWO_3 and the $\theta_w(M)$ oxides formed are discussed in terms of the ionic size of the M ions involved. It is suggested that M_xWO_3 bronzes are metastable if these M ions are small.

Introduction

The structural and physical effects of adding minor amounts of other metals to WO_3 have been much studied in the past and the phase fields associated with the bronze structures formed by nontransition elements have been carefully mapped (*1–3*). The same amount of interest has not been given to the phases obtained by the addition of a small amount of a transition element T to WO_3. Because of this a more systematic study of ternary T–W–O systems in the region close to WO_3 has been started by the present authors.

Among others, the behavior of the first transition elements is of obvious interest. In the case of Ti extensive crystallographic shear (*CS*) phase formation has been reported (*4*), whereas for the elements V (*5*) and Cr (*6*) no significant amounts of transition metal seem to enter into WO_3-like structures. For others of the 3*d* transition elements, T_xWO_3 bronzes with a perovskite-related structure have been observed to form, although the maximum x values in general are much lower than those found for the non-transition elements. For example, the highest observed x values for the bronzes Fe_xWO_3 (*7*, *8*), Co_xWO_3, and Ni_xWO_3 (*9*) are 0.0193, 0.035, and 0.040, respectively.

Of the 3*d* transition series, only the behavior of Mn in forming Mn_xWO_3 bronzes remains unknown, and it was therefore considered worthwhile to complete this area of investigation. Previous studies on the Mn–W–O system by Schröke (*10*) and by Trumm and

ISSN 0022–4596

Schröke (*11*) are mainly concerned with nonstoichiometric phases of the wolframite type in the phase regions near $MnWO_4$ and do not treat the region near WO_3, and especially the Mn_xWO_3 line of the phase diagram, in any detail. In addition, the discovery of an oxide with the Mo_5O_{14} structure in a number of other systems including Mn–W–O and Fe–W–O (*12*) has led us to reinvestigate the phase relationships in the Fe–W–O, Co–W–O, and Ni–W–O systems. Phase relations in Fe–W–O (*7*, *8*, *10*, *13*) are fairly well known, but neither the Co–W–O nor the Ni–W–O systems has been studied in depth near WO_3, although Phillips, Chang, and Scroger (*14*) have studied the more metal rich areas of the Co–W–O system in great detail at temperatures up to 1973°K.

The results of our findings are presented in this paper. Perovskite-related bronzes T_xWO_3 with small limiting x values were found only for Mn and Fe, as were oxide phases of the Mo_5O_{14} structure. These results are summarized on phase diagrams and are discussed in terms of the crystal chemistry of the 3*d* transition metal ions involved.

Experimental

The starting materials used were H_2WO_4 (Matheson, Coleman, and Bell), Mn_2O_3 (ICN. Pharm. Inc.), Fe_2O_3 (E. Merck, p.a.), NiO (Baker Analysed), Co_2O_3 (Baker Analysed), and CoO (p.a.). WO_3 was prepared by heating H_2WO_4 in air at about 1100°K for several days, and WO_2 was prepared from the trioxide by reduction in a stream of H_2/H_2O gas mixture at 1023°K. To obtain a suitable partial pressure of water the hydrogen gas was allowed to bubble through water kept at a temperature of 358°K. The tungsten oxides were checked by X-ray powder diffraction, and the dioxide was also checked by careful weighing before and after reduction.

Appropriate amounts of the oxides were thoroughly mixed and sealed in evacuated silica tubes or in Pt ampoules and heated at a temperature of 1373°K. The heating times ranged from 3 days up to 2 months. The longest time employed was usually 2 weeks but selected samples were heated for shorter or longer periods to check the stability of the phases observed. Particular attention was given the region near WO_3, and the majority of samples had gross compositions lying upon the T_xWO_3, $T_xW_{1-x}O_{2.80}$, $T_xWO_{2.80}$, and $T_xW_{1-x}O_{2.72}$ lines of the phase diagram. In addition some samples were prepared at other gross compositions, expecially along the $T_xW_{1-x}O_2$ line of the phase diagram, to clarify some aspects of the phase relations. Specimens with gross compositions within the Mn_xWO_3 bronze series were heated for 2–3 periods with intermittent grinding, to obtain a homogeneous bronze phase. After the heat treatment, all samples were quickly removed from the furnace, but no particular precautions were taken to quench them especially rapidly.

All samples were investigated by recording their X-ray powder patterns at room temperature with a Guinier–Hägg focusing camera using strictly monochromatic Cu$K\alpha_1$ radiation and KCl as an internal standard. The lattice parameters of phases characterized in this way were refined by least squares techniques, using programs written by Brandt and Nord (*15*). In addition, many samples were studied optically using a Zeiss Ultraphot microscope, and selected samples were examined in a JEM 100B electron microscope operating at 100 kV and fitted with a goniometer stage. Electron microscope specimens were prepared by crushing in an agate mortar under *n*-butanol and allowing a drop of the resultant suspension to dry on a net-like carbon film (*16*).

Results

Mn–W–O

The gross compositions of the samples prepared at 1373°K and the X-ray results thus obtained are presented in Table I. All these samples were heated for different times, but, in general, very little difference could be detected between those heated for 3–4 days or

TABLE I.

THE SAMPLES PREPARED IN THE Mn–W–O SYSTEM AT 1373°K[a, b]

Gross composition	Observed by X ray	Gross composition	Observed by X ray
$Mn_{0.002}WO_3$	M_1	$Mn_{0.005}W_{0.99}O_{2.82}$	θ_W(Mn), $MO_{2.82}$, (103-*CS*)
$Mn_{0.005}WO_3$	(M_1), M_2	$Mn_{0.005}W_{0.995}O_{2.80}$	θ_W(Mn), (($MO_{2.82}$))
$Mn_{0.008}WO_3$	M_2	$Mn_{0.01}W_{0.99}O_{2.80}$	θ_W(Mn), ($MO_{2.82}$)
$Mn_{0.010}WO_3$	M_2	$Mn_{0.02}W_{0.98}O_{2.80}$	θ_W(Mn), $MO_{2.82}$
$Mn_{0.013}WO_3$	*O*	$Mn_{0.03}W_{0.97}O_{2.80}$	$MO_{2.82}$, (θ_W(Mn)), (103-*CS*)
$Mn_{0.015}WO_3$	*O*	$Mn_{0.04}W_{0.96}O_{2.80}$	$MO_{2.82}$, 103-*CS*
$Mn_{0.020}WO_3$	*O*	$Mn_{0.005}WO_{2.80}$	θ_W(Mn)
$Mn_{0.022}WO_3$	*T*	$Mn_{0.01}WO_{2.80}$	$\theta_W(\mathrm{Mn})_1((W_{18}O_{49}))$
$Mn_{0.025}WO_3$	*T*	$Mn_{0.02}WO_{2.80}$	θ_W(Mn), ($W_{18}O_{49}$)
$Mn_{0.03}WO_3$	*T*, (($MnWO_4$))	$Mn_{0.03}WO_{2.80}$	θ_W(Mn), $W_{18}O_{49}$, (($MnWO_4$))
$Mn_{0.04}WO_3$	*T*, (($MnWO_4$)), (103-*CS*)	$Mn_{0.04}WO_{2.80}$	$W_{18}O_{49}$, θ_W(Mn), ($MnWO_4$)
$Mn_{0.05}WO_3$	*T*, 103-*CS*, ($MnWO_4$)	$Mn_{0.05}WO_{2.80}$	$W_{18}O_{49}$, (θ_W(Mn)), ($MnWO_4$)
$Mn_{0.06}WO_3$	103-*CS*, (*T*), ($MnWO_4$)	$Mn_{0.07}WO_{2.80}$	$W_{18}O_{49}$, ($MnWO_4$)
$Mn_{0.15}WO_3$	θ_W(Mn), $MnWO_4$	$Mn_{0.02}W_{0.98}O_{2.72}$	θ_W(Mn), $W_{18}O_{49}$
$Mn_{0.01}W_{0.99}O_{2.985}$	WO_3, (($MnWO_4$))	$Mn_{0.05}W_{0.95}O_{2.72}$	θ_W(Mn), ($MnWO_4$)
$Mn_{0.03}W_{0.97}O_{2.955}$	WO_3, ($MnWO_4$)	$Mn_{0.10}W_{0.90}O_{2.72}$	103-*CS*, ($MnWO_4$)
$Mn_{0.005}W_{0.995}O_{2.85}$	103-*CS*, $MO_{2.82}$,θ_W(Mn)	$Mn_{0.15}W_{0.85}O_{2.72}$	WO_3, $MnWO_4$
$Mn_{0.10}W_{0.90}O_{2.33}$	$W_{18}O_{49}$, WO_2, ($MnWO_4$)		
$Mn_{0.35}W_{0.65}O_{2.33}$	$MnWO_4$, WO_3		
$Mn_{0.50}W_{0.95}O_2$	WO_2, ($MnWO_4$)		
$Mn_{0.25}W_{0.75}O_2$	WO_2, $MnWO_4$		
$Mn_{0.45}W_{0.55}O_2$	$MnWO_4$, (WO_2)		
$Mn_{0.50}W_{0.50}O_2$	$MnWO_4$		
$Mn_{0.55}W_{0.45}O_2$	$MnWO_4$, ((Mn_3O_4))		

[a] The Guinier–Hägg X ray powder patterns have been obtained at room temperature.

[b] These results are also summarized in Fig. 1. The capital letters *M*, *O*, and *T* have been used to denote the monoclinic, orthorhombic, and tetragonal form of the Mn_xWO_3 bronze, respectively. The brackets () and (()) mean a small amount and a very small amount of a phase deducted from the X ray powder pattern intensity on the films.

for 2 weeks. These latter results are the ones presented in the table, and it thus appears that reaction proceeds rapidly at the temperature of 1373°K employed in this study. Many of the samples were also examined by optical microscopy and selected samples by electron microscopy. The results of all techniques employed were in accord with one another and are summarized on the phase diagram shown in Fig. 1.

Two particular areas of the phase diagram were studied with greatest attention. First, the region close to WO_3 and lying on the line Mn_xWO_3 ($0.002 \leq x \leq 0.06$) was chosen in order to clarify the question of the existence of a bronze phase. The results obtained by powder X-ray analysis show that a manganese tungsten bronze, Mn_xWO_3, was formed, with a very small homogeneity range extended in x, based on the fact that with increasing x value the symmetry changed in the sequence monoclinic → orthorhomic → tetragonal, as indicated in Table I.

As has been noted before, similar symmetry changes to these occur in WO_3 at high temperatures and can be preserved to room temperature by slight reduction, which produces a low density of *CS* planes in the WO_3 matrix (see Discussion). Thus, in order to be certain that a bronze is formed the crystals were also examined by transmission electron microscopy. This revealed that crystal frag-

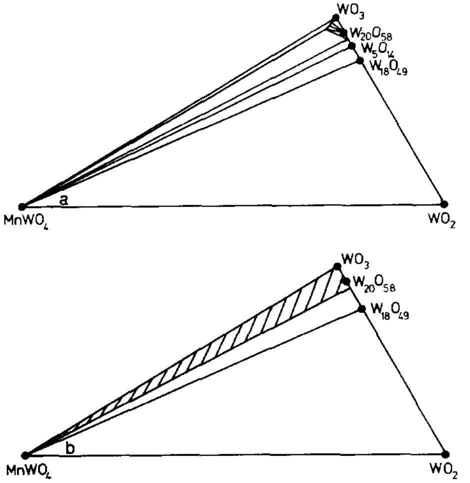

FIG. 1. (a) Nonequilibrium phase diagram obtained after heating at 1373°K for times ranging from a few days to a couple of weeks. The phase region $MO_{2.80}$–$MO_{2.90}$, close to the binary tungsten oxide line, is complex with disordered {103} *CS* structures at higher oxygen compositions and other disordered structures at lower oxygen compositions. Prolonged heating for extended periods of times results in the decomposition of these latter compounds and the phase diagram thus obtained is exemplified in (b).

ments were generally free of *CS* planes and to a good approximation each sample resembled WO_3 in electron-diffraction contrast.

The changes in the lattice parameters of the bronze are plotted in Fig. 2. It can be seen from these samples, studied at room temperature, that within the interval $0 \leq x \lesssim 0.012$ a monoclinic bronze isotypic with the monoclinic form of WO_3 is found. The sample with $x = 0.005$ appeared, however, to contain two monoclinic forms with a small shift in the lattice parameters. Between $0.012 \leqslant x \leqslant 0.020$ and $0.020 \leqslant x \leqslant 0.027$, respectively, the orthorhombic and tetragonal forms are found. Several of the short-time heated manganese bronze samples were also heated for another period of 2 months, and in these samples no clear X-ray evidence for a decomposition of the bronze to other oxides was observed. However, weak diffuse bands that are usually associated with a high number of disordered *CS* planes in the WO_3 structure appeared on the X-ray diagrams and suggest decomposition may be incipient.

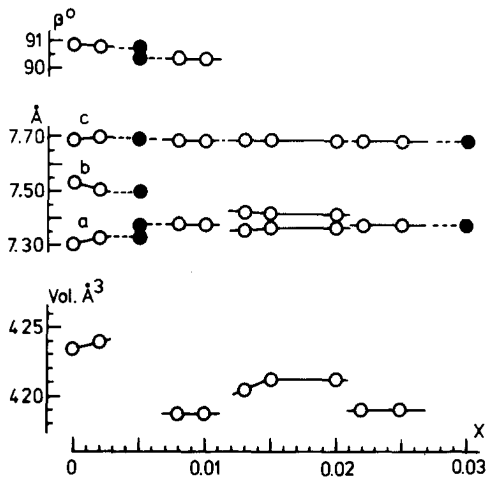

FIG. 2. Unit cell parameters at room temperature versus composition x for the bronze Mn_xWO_3. In the figure the parameters $a = 2^{1/2}. a_T$ and $c = 2. c_T$ has been plotted for the tetragonal form, where a_T and c_T are the crystallographic unit cell parameters. Open circles refer to monophasic samples and filled circles to multiphasic samples.

So far these phases have not been studied extensively to see whether they possess other typical bronze-like properties. To date, only preliminary measurements of the magnetic properties have been made, but these show that a Curie–Weiss law is followed (*17*) and that manganese is present as the Mn^{2+} ion. An extended study of the physical properties is planned and will be presented in the future.

The second area of interest was the region lying close to $WO_{2.80}$ and along the $Mn_xW_{1-x}O_{2.80}$ and $Mn_xWO_{2.80}$ lines in the phase diagram. In this area we have found that an oxide isostructural with the binary θ-molybdenum oxide, Mo_5O_{14}, forms. This oxide will subsequently be denoted θ_W(Mn) oxide, to correspond with other ternary θ-oxide phases found to have this structure type (*12*). The results obtained showed that at most only a very small amount of manganese is found in the θ_W(Mn) oxide (cf. Table I). For instance, no manganese seems to be substituted for tungsten, even to a small extent, as the

$Mn_{0.005}W_{0.995}O_{2.80}$ sample clearly contains other oxides. No significant amount of manganese seems to enter either the tunnels or cages found in the Mo_5O_{14} structure, as would be expected for a bronze-like phase with an existence region along the $Mn_xW_{2.80}$ line. Thus, this oxide may be considered as being a pseudobinary W_5O_{14} oxide from this point of view, although the presence of about 0.5 at.% manganese in the structure cannot be completely excluded. The tetragonal unit cell parameters for the oxide, which did not vary significantly from one sample to another, were $a = 2.3284(\pm 3)$ nm and $c = 0.3793(\pm 1)$ nm. Some samples of the $\theta_W(Mn)$ oxide were heated for an additional period of 2 months, and in these samples it was clearly found that prolonged heating for this extended time made the oxide decompose into {103} *CS* oxides and $W_{18}O_{49}$.

For the $W_{18}O_{49}$, WO_2, and $MnWO_4$ oxides no extended homogeneity ranges could be detected. As can be seen in Table I additional oxides were found in the preparations $Mn_{0.02}W_{0.98}O_{2.72}$, $Mn_{0.05}W_{0.95}O_2$, and $Mn_{0.45}W_{0.55}O_2$. This was also true for a sample of gross composition $Mn_{0.55}W_{0.45}O_2$, where the ampoules contained a pressure of oxygen gas released by the decomposition of unstable manganese oxides. Moreover, the lattice parameters of the $W_{18}O_{49}$, WO_2, or $MnWO_4$ oxides found in these and other samples were not significantly different from the stoichiometric oxides themselves (*18–20*). However, it should be remembered that we cannot, from these data, exclude the possibility that a very small amount of Mn is able to substitute for W in these oxides.

The final result to mention concerns samples with overall compositions in the region $(Mn,W)O_{2.80}$ to $(Mn,W)O_{2.85}$. X-ray powder patterns indicated the presence of an additional phase, characterized by diffuse superstructure lines, and indicating the presence of a pseudocubic disordered ReO_3-like structure. Electron microscopy coupled with studies in other systems, notably the Ge–W–O system (*21*) and the binary W–O system (*22*), have shown that the phase consists of very disordered crystals of an oxide with a composition close to $WO_{2.82}$. The structure of this phase is so far unknown. Heating samples containing this oxide for long periods of time showed that it decomposed in a similar fashion to the $\theta_W(Mn)$ oxide.

Fe–W–O, Co–W–O, and Ni–W–O

As these systems were examined in rather less detail than the Mn–W–O system, we will present only a summary of our results here. The results obtained after long heating times were quite straightforward and are illustrated in the phase diagrams shown in Fig. 3. Thus, after prolonged heating, the only ternary phases that remain stable are the tungstates $FeWO_4$, Fe_2WO_6, $CoWO_4$, and $NiWO_4$. No attempt was made to map out the existence ranges of these oxides, and in the phase area of interest to us they were treated as line phases. In the $Ni_xW_{1-x}O_2$ system a two-phase line in the ternary system between $W_{18}O_{49}$ and a much more reduced phase intersects the dioxide line at about $x = 0.20$ (see Fig. 3c). The new phase was present in a very small amount and no effort was made to identify it.

We found by X-ray analysis no evidence that Fe, Co, or Ni was able to substitute in any significant amounts for W in the binary tungsten oxides. The lattice parameters of $W_{18}O_{49}$ and WO_2 were not very different parameters of the binary oxides and in addition the samples with more than a couple of atomic percent of ternary metal contained other oxide phases.

When heating times of 1 to 2 weeks were employed, the phase relations in the region near to WO_3 were found to be more complex, and several other metastable phases were observed, including the bronze phase Fe_xWO_3, $\theta_W(M)$oxide phases, and the $MO_{2.82}$ phase. These will be described in turn.

M_xWO_3 Bronzes

An Fe_xWO_3 bronze was found which was somewhat similar to the Mn_xWO_3 bronze described above. The Fe_xWO_3 bronze was,

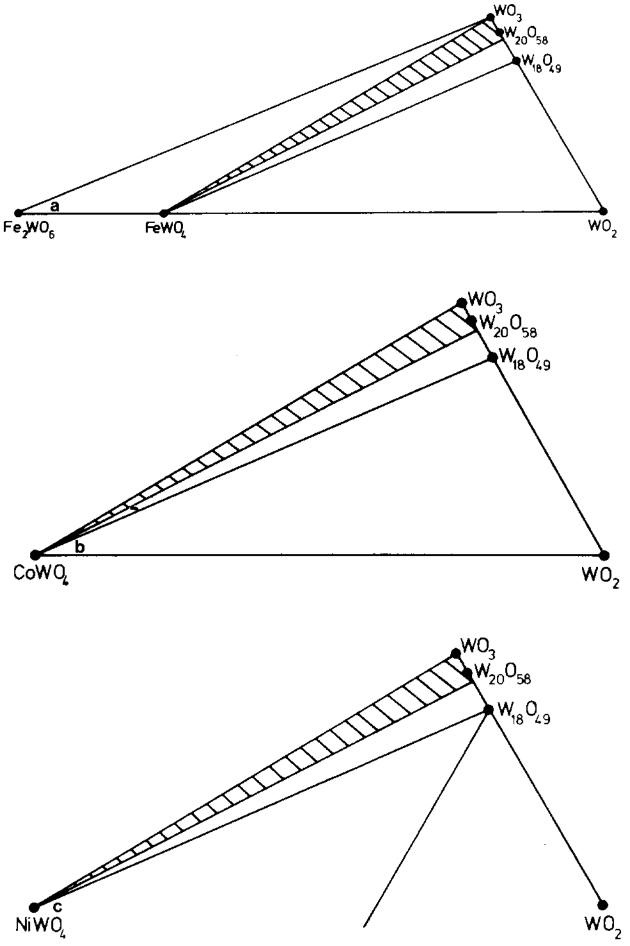

FIG. 3. Equilibrium phase diagrams for (a) the Fe–W–O, (b) the Co–W–O, and (c) the Ni–W–O, systems at 1373°K.

however, only rarely found to be monophasic and X-ray photographs of compositions within the previously reported bronze range (*7*, *8*) usually showed either a mixture of bronze phases of different symmetries or bronze phases coexisting with other oxides. These other products varied both with overall composition and with heating time, and it was apparent that the Fe_xWO_3 bronze decomposed at a significant rate.

Attempts to prepare the Co_xWO_3 and Ni_xWO_3 bronzes at 1373°K failed, although these phases have been reported to form at somewhat lower temperatures (*9*). Instead the equilibrium was found to be between the appropriate binary tungsten oxide and the corresponding tungstates. At gross compositions close to WO_3, the high-temperature forms of the trioxide were observed to be partly quenched to room temperature.

$\theta_W(M)$ Oxides

As in the case of the T_xWO_3 bronzes, the Fe–W–O system was most similar in behavior to the Mn–W–O system, and a θ_W(Fe) oxide was readily prepared. The tetragonal unit cell parameters did not vary appreciably from one sample to another and were found to be $a = 2.329(\pm 5)$ nm and $c = 0.03794(\pm 1)$ nm. In addition, the samples of gross composition

$Fe_{0.01}W_{0.99}O_{2.80}$ and $Fe_{0.01}WO_{2.80}$ clearly contained other phases as revealed by X-ray analysis, implying that the θ_W(Fe) oxide contains only very small amounts of iron. As with the θ_W(Mn) oxide, it decomposes upon prolonged heating and at a rate significantly higher than the corresponding θ_W(Mn) phase.

This trend was continued in the Co and Ni systems. A θ_W(Co) oxide was only rarely present in small amounts in some samples and no θ_W(Ni) oxide was ever observed.

(T, *W*)$O_{\sim 2.82}$ *Oxides*

Disordered (T,W)$O_{\sim 2.82}$ oxides were found in all three systems. In each of them the phase was metastable and decomposed to the phases shown in Fig. 3.

Discussion

The Existence of Mn_xWO_3 *and* Fe_xWO_3 *Bronzes*

In recent investigations of ternary T–W–O systems, particularly V–W–O (*5*) and Nb–W–O and Ta–W–O (*23*), we have found that the high-temperature forms of WO_3 can be retained to room temperature. This appears to be associated with the presence of {102} *CS* planes in the slightly reduced trioxide crystal matrix. The first point to ascertain, therefore, is whether T_xWO_3 bronzes really form in the Mn–W–O and Fe–W–O systems, as in the past bronze formation at low x values has invariably been inferred from symmetry changes in the WO_3 lattice.

In the Fe_xWO_3 case, the existence of a bronze phase seems reasonably certain, as Mössbauer experiments have indicated the presence of Fe^{2+} in the structure in sites which are not of octahedral symmetry (*7*, *8*). In the Mn_xWO_3 case the evidence is to some extent indirect. In our experience these high-temperature forms of WO_3 have never been found as monophasic samples but always coexist with significant amounts of the normal room-temperature monclinic form. Such samples also contain a relatively high density of {102} *CS* planes, and we have supposed that regions of crystal with high densities of *CS* planes stabilize the high-temperature forms to room temperatures while regions of crystal with low *CS* plane densities are not stabilized and are monoclinic. The samples in general contain a very uneven distribution of *CS* planes in accord with this hypothesis. The fact that homogeneous samples were obtained in the Mn_xWO_3 system therefore suggests that a genuine bronze phase forms. In addition to this, electron microscope analysis of genuine bronze phases, as found in the Zr_xWO_3 system for example (*24*, *25*), show that crystal fragments are almost completely free of *CS* planes. The electron microscope studies of the Mn_xWO_3 samples in the bronze region also show very few *CS* planes, certainly not enough to account for the stoichiometry changes involved. We are thus confident that a bronze phase is formed here. Associated studies of the physical and chemical properties of these materials to determine the extent to which they possess other bronze-like properties are underway and will be reported in the future.

For much the same reasons as those given above, we have also supposed that no bronze is present in the Co–W–O and Ni–W–O systems at the temperature of our preparations, 1373°K, after a heating time of 1 week.

T_xWO_3 *Stability*

There seems to be a definite trend in the stability of the perovskite bronze T_xWO_3 formed (where x is small, and of the order of a few atomic percent) as we pass along the series from the left-hand side of the periodic table to the right. Thus, neither Ti (*4*), V (*5*), or Cr (*6*) form perovskite bronzes with small x values; Mn forms a relatively stable bronze, but our experiments suggest that it is perhaps starting to decompose after 2 months of heating; Fe forms a bronze which decomposes after a week or so; while Co and Ni form bronzes at lower temperatures (*9*) but do not form bronzes which are stable for 1 week at 1373°K. Similarly, Zr_xWO_3 slowly decomposes (*25*) while Ge_xWO_3 is stable only at temperatures of the order of 800°K (*26*).

There is no doubt that this behavior can be correlated with ionic size (*27*) with small atoms ending to prefer tetrahedral or octahedral coordination, while larger atoms such as Na are better able to tolerate the coordination provided by the cage sites in between the WO_6 octahedra which make up the structure of WO_3. When considering the 3*d* transition elements one is faced with a number of problems in assessing an ionic size to use. First a radius appropriate to the cage site in the WO_3 structure is not available for these ions and second a great deal of doubt exists over which ionic state of the metal atom T is present in these oxides. As far as this latter point is concerned, it is a generally accepted empirical rule that the lowest available valence of the metal T is most appropriate to describe its ionic state in the tungsten bronzes, and this is substantiated by the knowledge that both Mn (*17*) and Fe (*7, 8*) are in the divalent state. Thus, in Fig. 4, we have plotted some of the ionic radii of these ions, including the high-spin radii for octahedral coordination, as experimental results suggest that this state is more likely to hold for these ions in oxide lattices (*28*).

For the ions we are principally concerned with, Mn^{2+}, Fe^{2+}, Co^{2+}, and Ni^{2+}, the ionic radii are in the order $Mn^{2+} > Fe^{2+} > Co^{2+} > Ni^{2+}$, which parallels the stability noted for the T_xWO_3 bronzes. When we consider the ions of Ti, V, and Cr more qualitative considerations arise, as the T^{2+} ionic state is not well defined in oxide lattices. Ti^{2+} and V^{2+} nominally occur in the metallic TiO_x and VO_x nonstoichiometric monoxides, but CrO is unknown. If this ionic state were stabilized in the bronzes, one would expect Ti_xWO_3, V_xWO_3, and Cr_xWO_3 to form on the basis of ionic size. Since these bronzes do not form the conclusion is that higher ionic states are in fact present. This is supported by phase equilibria on the MO_2 line of the phase diagrams, for while in the case of Mn, Co and Ni the divalent $T^{2+}WO_4$ tungstate forms, in the Ti–W–O system $(Ti_xW_{1-x})O_2$ forms with Ti being nominally quadrivalent, while both V and Cr form oxides $T_2^{3+}WO_6$ with trivalent ions. Thus we would anticipate Ti^{4+} V^{3+} and Cr^{3+} to be the most favored species in this half of the 3*d* series. The small size of these ions, as shown in Fig. 4, suggests that any T_xWO_3 bronze formed would be of very small stability, although the use of short heating times and low temperatures may yield evidence of the transitory appearance of this structure type.

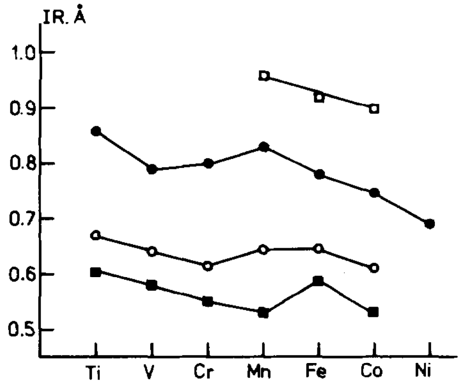

FIG. 4. Ionic radii of the 3*d* transition metals, after Shannon (*30*). For octahedral cations the high-spin values are shown. The symbols represent, □, M^{2+} ions in eight-fold coordination; ●, M^{2+} ions in octahedral coordination; O, M^{3+} ions in octahedral coordination; ■, M^{4+} ions in octahedral coordination.

$\theta_W(M)$ Oxides

The trend in the formation and stability of the $\theta_W(T)$ phase is very similar to that found for the T_xWO_3 bronzes. Thus, although the X-ray results suggest the amount of Mn or Fe in the oxide is small and that the ternary metal does not form a large part of the structure, it seems to play an important role in the stability of this phase. This can possibly arise in a number of ways. For instance, it is possible to suppose that the presence of T^{2+} ions in some of the tunnels in the θ_W structure could partially stabilize it, and thus one would expect that large ions would be most effective here. This is reasonable in view of the fact that large ions in general are more effective in forming the θ_W phase than small ions (*12*) and that the only elements of the 3*d* transition series to form a θ_W oxide are the two with the largest ionic radii. If only one metal atom per unit cell of the θ_W phase is needed for this stabilization, then about 2.5 at.% of the metal T would be present, while if the metal had only to be present in next-nearest-neighbor unit cells the amount would fall subsequently. Such small amounts of interpolated metal appear to be sufficient to stabilize the T_xWO_3 phases.

This is not the only possibility. There is no doubt that the θ_W oxides form via a vapor reaction in our experiments (*27*). It is possible that in the initial reaction unit cells of the θ_W oxide are laid down with a high concentration of stabilizing ions in them. For example one ion in each empty tunnel would require about 20 at% of T. However, further crystal growth may then proceed on this template with only occasional inclusion of T ions in a predominantly tungsten–oxygen framework. Such ions may be distributed at random, or may be rejected by the growing crystal until sufficient are present on the surface to form another layer of unit cells with filled tunnels. Such a mechanism has been suggested for the presence of faulting in Nb_2O_5-related block structures by Anderson, Browne, and Hutchison (*29*). In either case crystals with very low overall concentrations of T ions would result. Other possibilities may also exist to explain the formation of the θ_W oxide. With respect to our present considerations, it would seem likely that the relatively small Mn^{2+} and Fe^{2+} ions would prefer octahedral coordination and that the θ_W oxide would decompose to TWO_4 tunstates in an analogous way to the T_xWO_3 bronzes.

$(T, W)O_{\sim 2.82}$ *Oxide*

Unlike the T_xWO_3 and θ_W phases this oxide occurs both in the binary system and in all the ternary systems studied here. This may, in fact, mean that it is a binary oxide, although the severe disorder of the material and the resulting poor X-ray diagrams do not eliminate the possibility of it being a nonstoichiometric phase with an existence region within the ternary areas of the phase diagrams. The lack of precise experimental data on this point suggests that any speculation would be better postponed.

Acknowledgments

One of the authors (R.J.D.T.) is grateful to the Science Research Council for an equipment grant. The research has also been performed within a program supported by the Swedish Natural Science Research Council (T.E.).

References

1. P. G. Dickens and M. S. Whittingham, *Quart. Rev.* **22**, 30 (1968).
2. P. G. Dickens and P. J. Wiseman, *in* "Inorganic Chemistry, Series Two" (L. E. J. Roberts, Ed.), Vol. 10, Butterworths, London.
3. P. Hagenmuller, "Comprehensive Inorganic Chemistry," (J. C. Bailar *et al.*, Eds.), Vol. 4, Pergamon Press, New York (1973).
4. T. Ekström and R. J. D. Tilley, *Mater. Res. Bull.* **9**, 705 (1974).
5. T. Ekström and R. J. D. Tilley, *J. Solid State Chem.* **16**, 141 (1976).
6. T. Ekström and R. J. D. Tilley, *Mater. Res. Bull.* **10**, 1175 (1975).
7. I. J. McColm, R. J. D. Tilley, C. P. M. Barton, and N. N. Greenwood, *J. Solid State Chem.* **16**, 265 (1976).
8. J. P. Doumerc, G. Schiffmaker, P. Caro, and M. Pouchard, *C.R. Acad. Sci. Paris, Ser. C* **282C**, 295 (1976).
9. M. Pouchard, J. P. Chaminade, J. P. Doumerc, J. C. Launay, and P. H. Hagenmuller, *Mater. Res. Bull.* **7**, 223 (1972).
10. H. Schröcke, *Neues Jahrb. Miner. Abh.* **110**, 115 (1969).
11. A. Trumm and H. Schröke, *Z. Phys. Chem. (NF)* **99**, 171 (1976).
12. Thommy Ekström and R. J. D Tilley, *J. Solid State. Chem.* **19**, 125 (1976).
13. N. E. Schmahl and H. Dillenberg, *Z. Phys. Chem.* (NF) **77**, 113 (1972).
14. B. Phillips, L. L. Y. Chang, and M. G. Scroger, *Trans. Met. Soc. AIME* **233**, 1220 (1976).
15. B. G. Brandt and A. G. Nord, *Chem. Commun. Univ. Stockholm*, N. 5 (1970).
16. J. R. Gannon and R. J. D. Tilley, *J. Microsc.* **106**, 59 (1976).
17. B. Blom, private communication.
18. Thommy Ekström, *Chem. Commun. Univ. Stockholm*, No. 7 (1975).
19. A. Magnéli and G. Anderson, *Acta Chem. Scand.* **11**, 1635 (1958).
20. ASTM index, card number 13-434.

21. THOMMY EKSTRÖM, E. IGUCHI, AND R. J. D. TILLEY, to be published.

22. R. PICKERING AND R. J. D. TILLEY, *J. Solid State Chem.* **16**, 247 (1976).

23. THOMMY EKSTRÖM AND R. J. D. TILLEY, *J. Solid State Chem.* **18**, 123 (1976).

24. THOMMY EKSTRÖM AND R. J. D. TILLEY, *Mater. Res. Bull.* **9**, 999 (1974).

25. THOMMY EKSTRÖM AND R. J. D. TILLEY, *J. Solid State Chem.* **17**, 227 (1976).

26. M PARMENTIER AND C. GLEITZER, *J. Solid State Chem.* **17**, 255 (1976).

27. THOMMY EKSTRÖM AND R. J. D. TILLEY, to be published.

28. C. J. BALLHAUSEN, "Ligand Field Theory," Chap. 10. McGraw–Hill, New York (1962).

29. J. S. ANDERSON, J. M. BROWNE, AND J. L. HUTCHISON, *Nature* **273**, 151 (1972).

30. R. D. SHANNON, *Acta Crystallogr. Sect. A* **32**, 751 (1976).